

Fuzzy-rule-embedded Reduction Image Construction Method for Image Enlargement with High Magnification

Hakaru Tamukoh¹, Noriaki Suetake², Hideaki Kawano³, Ryosuke Kubota⁴, Byungki Cha⁵ and Takashi Aso⁵

¹Graduate School of Life Science and Systems Engineering, Kyushu Institute of Technology, Kyushu, Japan

²Graduate School of Science and Engineering, Yamaguchi University, Yamaguchi, Japan

³Graduate School of Engineering, Kyushu Institute of Technology, Kyushu, Japan

⁴Department of Intelligent System Engineering, Ube National College of Technology, Ube, Japan

⁵Faculty of Management and Information Sciences, Kyushu Institute of Information Sciences, Kyushu, Japan

Keywords: Image Enlargement, Image Reduction, Data Embedding, Fuzzy Inference.

Abstract: This paper proposes a fuzzy-rule-embedded reduction image construction method for image enlargement. A fuzzy rule is generated by considering distribution of pixel value around a target pixel. The generated rule is embedded into the target pixel in a reduction image. The embedded fuzzy rule is used in a fuzzy inference to generate a highly magnified image from the reduction image. Experimental results, which scale factors are three and four, show that the proposed method realizes high-quality image enlargement in terms of both objective and subjective evaluations in comparison with conventional methods.

1 INTRODUCTION

In recent years, high-resolution displays have become widely used such as high-definition televisions, mobile devices and smart phones. In addition, a 4K (3840×2160 pixels) resolution already exist in digital television and digital cinematography, and an 8K (7680×4320 pixels) resolution will be available as ultra-high-definition displays in the near future. At the same time, people can obtain over giga-pixel images, because high-resolution digital cameras are widely commoditized. In addition, image- and video-sharing services become as common all over the world. To upload image or video to these services, people have to reduce image size into less than quarter size. Naturally, users require browsing high-resolution images on the high-resolution displays. To satisfy this requirement, whole or part of image have to be enlarged larger than four times in size.

Image reduction and enlargement methods are very important technologies in sharing and displaying images among such devices. Classical image scaling methods—such as nearest neighbor interpolation (NNI), bilinear interpolation (BLI), and bicubic Interpolation (BCI)—are based on interpolation using kernels (Lin, 1990), (Keys, 1981). These interpolation-based methods achieve fast smooth image reduction and enlargement; however, once images

are reduced by these methods, they cannot restore the high-frequency image components lost in the reduction process, and therefore cannot preserve clearly the step edges and peaks of an image. This is caused by the fact that the high-frequency image components beyond the Nyquist frequency cannot be restored using these simple kernel-based methods. If multiple images are available, a high-resolution image can be generated from a set of low-resolution images in the same scene (Farsiu et al., 2004), but they cannot be applied to stationary images. To address this problem, various advanced image enlargement methods from the single image accompanying the estimation of the high-frequency component have been proposed (Greenspan et al., 2000), (Siu and Hung, 2012). The estimated high-frequency component is overlapped with a blurred image generated by interpolation based methods, to generate a high-quality image. However, estimation of high-frequency component is difficult when scale factor is over three or four.

In this paper, we propose a fuzzy-rule-embedded image construction method to generate a reduction-image in the image reduction process. The embedded fuzzy rules are used in the proposed fuzzy inference to generate an enlarged image with high magnification in the image enlargement process. To show the effectiveness of the proposed method, we compare results of the proposed method with the conventional meth-

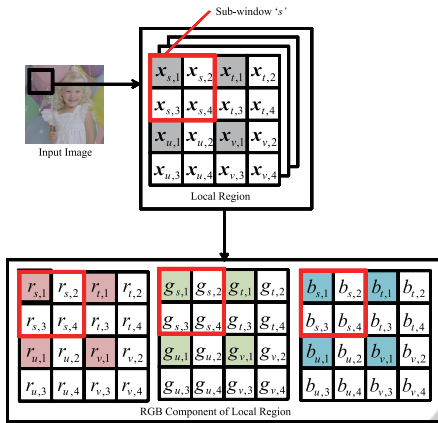


Figure 1: Definition of signals in this study.

ods under the subjective and objective evaluation.

2 FUNDAMENTAL METHOD

In this section, we explain a fundamental method (Tamukoh et al., 2013) of a data embedding to introduce an idea of proposed method easily.

Figure 1 shows a definition of signals for the proposed method. The local region consists of 16 pixels and they are divided into 4 sub-windows $s, t, u,$ and v . In the proposed method, the sub-window s is defined as a focused window. Each sub-window has one actual pixel which is denoted by index '1', and the other 3 pixels are interpolation target pixels which are denoted by index '2', '3' and '4'. Each pixel has 3 color components $r, g,$ and $b,$ and each color component is represented by 8 bit accuracy.

Both of an image reduction and an enlargement process are based on NNI. If information on interpolation target pixels can be embedded into the actual pixel in the image reduction process, we can utilize that information for high-quality enlargement in the image enlargement process.

2.1 Image Reduction Process

In this subsection, we explain about an image reduction process and a data embedding method.

First, we select representative pixels $k_j^*, (j = 2, 3, 4)$ for interpolation target pixels $(\vec{x}_{s,2}, \vec{x}_{s,3}, \vec{x}_{s,4})$ in the focused window. The k_j^* is calculated by Eq.(1).

$$k_j^* = \begin{cases} \underset{k \in (s,t)}{\operatorname{argmin}} \|\vec{x}_{k,1} - \vec{x}_{s,j}\| & j = 2 \\ \underset{k \in (s,u)}{\operatorname{argmin}} \|\vec{x}_{k,1} - \vec{x}_{s,j}\| & j = 3 \\ \underset{k \in (s,t,u,v)}{\operatorname{argmin}} \|\vec{x}_{k,1} - \vec{x}_{s,j}\| & j = 4 \end{cases} \quad (1)$$

$$\begin{aligned} p_{(k_2^*)} &= \underline{1} \\ p_{(k_3^*)} &= \underline{0} \\ p_{(k_4^*)} &= \underline{11} \\ r'_{s,1} &= 11100001 \\ g'_{s,1} &= 10000001 \\ b'_{s,1} &= 01101010 \end{aligned} \xrightarrow{\text{Data embedding}} \begin{aligned} \tilde{r}'_{s,1} &= 11100001 \\ \tilde{g}'_{s,1} &= 10000000 \\ \tilde{b}'_{s,1} &= 01101011 \end{aligned}$$

Figure 2: Data embedding scheme of fundamental method.

Then, a place code $p_{(k_j^*)}$ is calculated by following equations based on the representative pixel k_j^* .

$$p_{(k_2^*)} = \begin{cases} 0 & k_2^* = s \\ 1 & k_2^* = t \end{cases}, \quad (2)$$

$$p_{(k_3^*)} = \begin{cases} 0 & k_3^* = s \\ 1 & k_3^* = u \end{cases}, \quad (3)$$

$$p_{(k_4^*)} = \begin{cases} 00 & k_4^* = s \\ 01 & k_4^* = t \\ 10 & k_4^* = u \\ 11 & k_4^* = v \end{cases}. \quad (4)$$

Each code $p_{(k_j^*)}$ is represented as binary number.

Finally, the place code $p_{(k_j^*)}$ is embedded into RGB component of the actual pixel $\vec{x}_{s,1}$. Figure 2 shows a data embedding scheme of fundamental method. Each color component of actual pixel is represented as binary number $r'_{s,1}, g'_{s,1}, b'_{s,1}$. The place code $p_{(k_2^*)}$ and $p_{(k_3^*)}$ are embedded into the lowest bit of $r'_{s,1}$ and $g'_{s,1}$ component, respectively. Similarly, the code $p_{(k_4^*)}$ is embedded into lower two bit of $b'_{s,1}$ component. By processing of the proposed data embedding method, losses of R and G component on the actual pixel are one bit, and loss of B component is two bit. However, these losses affect quite few changes to the image, because the maximum error is up to three in the range of 0 to 255 if lower two bit of the B component is fully inverted.

After the data embedding, by the factor of 0.5 image reduction is applied to the embedded image using NNI, a data-embedded reduction image is obtained.

2.2 Image Enlargement Process

In this subsection, we explain about an image enlargement process and an interpolation scheme using the data-embedded reduction image.

First, the local region of 2×2 pixels is extracted from the data-embedded reduction image. Then, the factor of two image enlargement is applied to the extracted pixels using NNI. The definition of signals

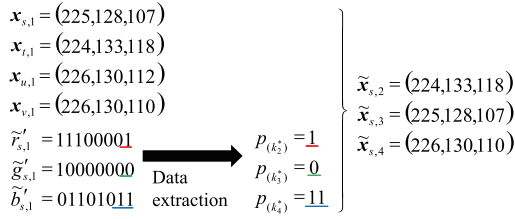


Figure 3: Interpolation scheme of fundamental method based on the embedded information.

is also shown in Fig.1 as same as the image reduction process. In the enlargement process, white pixels in Fig.1 are defined as interpolation target pixels ($\tilde{\vec{x}}_{s,2}, \tilde{\vec{x}}_{s,3}, \tilde{\vec{x}}_{s,4}$).

Next, the embedded place code is extracted from RGB components ($r_{s,1}, g_{s,1}, b_{s,1}$) of actual pixel $\vec{x}_{s,1}$. In particular, place codes $p(k_2^*), p(k_3^*)$ are extracted from the lowest bit of $r'_{s,1}, g'_{s,1}$ components, respectively. Similarly, the place code $p(k_4^*)$ is also extracted from lower 2 bit of $b'_{s,1}$ component.

Then, interpolation target pixels ($\tilde{\vec{x}}_{s,2}, \tilde{\vec{x}}_{s,3}, \tilde{\vec{x}}_{s,4}$) are interpolated by the following equations based on the extracted place codes.

$$\tilde{\vec{x}}_{s,2} = \begin{cases} \vec{x}_{s,1} & p(k_2^*) = 0 \\ \vec{x}_{t,1} & p(k_2^*) = 1 \end{cases}, \quad (5)$$

$$\tilde{\vec{x}}_{s,3} = \begin{cases} \vec{x}_{s,1} & p(k_3^*) = 0 \\ \vec{x}_{u,1} & p(k_3^*) = 1 \end{cases}, \quad (6)$$

$$\tilde{\vec{x}}_{s,4} = \begin{cases} \vec{x}_{s,1} & p(k_4^*) = 00 \\ \vec{x}_{t,1} & p(k_4^*) = 01 \\ \vec{x}_{u,1} & p(k_4^*) = 10 \\ \vec{x}_{v,1} & p(k_4^*) = 11 \end{cases}. \quad (7)$$

Figure 3 shows a scheme of proposed interpolation method. Interpolation target pixels ($\tilde{\vec{x}}_{s,2}, \tilde{\vec{x}}_{s,3}, \tilde{\vec{x}}_{s,4}$) copy the representative pixel to itself selected from $\vec{x}_{s,1}, \vec{x}_{t,1}, \vec{x}_{u,1}, \vec{x}_{v,1}$ based on the extracted place code $p(k_2^*), p(k_3^*)$ and $p(k_4^*)$.

Finally, the lower 2 bit of B component changes its value to "10". This finalize process minimizes an average error of data embedding effect.

The fundamental method directly copies the representative pixel to the interpolation target pixel, thus, it obtains better quality enlarged image than the ordinary NNI. However, the fundamental method can be applied to the factor of two only, and image artifact is occasionally generated around edge region.

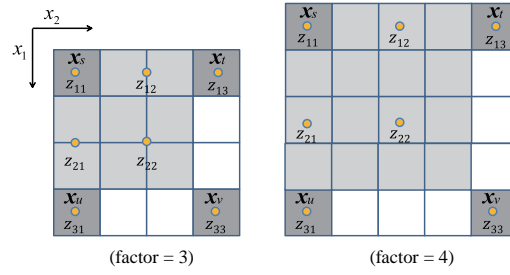


Figure 4: Pixel coordinates and output values assignment on fuzzy rules.

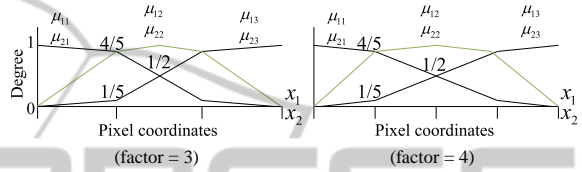


Figure 5: Membership functions.

3 PROPOSED METHOD

In this section, we propose a fuzzy-rule-embedded reduction image construction method by extending the fundamental method. The basic idea of fuzzy rule embedding is same as the data embedding of fundamental method. In the proposed method, we embed fuzzy rules as data. The embedded fuzzy rules are used in a fuzzy inference to generate an enlarged image with high magnification.

We introduce a set of fuzzy rule for image enlargement as shown in Eq.8.

$$\begin{aligned}
 & \text{if } x_1 \text{ is } \mu_{11} \text{ and } x_2 \text{ is } \mu_{21}, \text{ then } y \text{ is } z_{11} = \vec{x}_s, \\
 & \text{if } x_1 \text{ is } \mu_{11} \text{ and } x_2 \text{ is } \mu_{22}, \text{ then } y \text{ is } z_{12}, \\
 & \text{if } x_1 \text{ is } \mu_{11} \text{ and } x_2 \text{ is } \mu_{23}, \text{ then } y \text{ is } z_{13} = \vec{x}_t, \\
 & \text{if } x_1 \text{ is } \mu_{12} \text{ and } x_2 \text{ is } \mu_{21}, \text{ then } y \text{ is } z_{21}, \\
 & \text{if } x_1 \text{ is } \mu_{12} \text{ and } x_2 \text{ is } \mu_{22}, \text{ then } y \text{ is } z_{22}, \\
 & \text{if } x_1 \text{ is } \mu_{13} \text{ and } x_2 \text{ is } \mu_{21}, \text{ then } y \text{ is } z_{31} = \vec{x}_u, \\
 & \text{if } x_1 \text{ is } \mu_{13} \text{ and } x_2 \text{ is } \mu_{23}, \text{ then } y \text{ is } z_{33} = \vec{x}_v,
 \end{aligned} \quad (8)$$

where, x_1 and x_2 represent pixel coordinates as shown in Fig.4. Membership functions μ_{ij} ($i = 1, 2, 3; j = 1, 2, 3$) are defined in Fig.5. Output of fuzzy rules are assigned as shown in Fig.4. Here, dark gray pixels are given from the reduction image, and light gray pixels are interpolation target in the enlargement process.

In the proposed fuzzy rules Eq.8, outputs z_{11}, z_{13}, z_{31} and z_{33} can be assigned from the given pixel value. On the other hands, rest of three outputs z_{12}, z_{21} and z_{22} should be calculated in the image reduction process same as the fundamental method.

3.1 Image Reduction Process

Outputs of proposed fuzzy rules z_{12} , z_{21} and z_{22} are calculated by following equation.

$$\begin{pmatrix} k_{z_{12}}^* \\ k_{z_{21}}^* \\ k_{z_{22}}^* \end{pmatrix} = \begin{cases} \operatorname{argmin}_{k \in (0,1,2,3)} \|\vec{x}_s + \frac{k}{3}(\vec{x}_t - \vec{x}_s) - \Psi_{12}\| \\ \operatorname{argmin}_{k \in (0,1,2,3)} \|\vec{x}_s + \frac{k}{3}(\vec{x}_u - \vec{x}_s) - \Psi_{21}\| \\ \operatorname{argmin}_{k \in (0,1,2,3)} \|\vec{x}_s + \frac{k}{3}(\vec{x}_v - \vec{x}_s) - \Psi_{22}\| \end{cases}, \quad (9)$$

where, Ψ_{12} , Ψ_{21} , and Ψ_{22} represent virtual pixel values at pixel coordinates of z_{12} , z_{21} and z_{22} . For instance, Ψ_{22} is calculated by the average of around four pixels at pixel coordinates of z_{22} in the case of factor three, and is directly copied from that of pixel value in the case of factor four, shown in Fig.4.

After calculated Eq.9, a fuzzy rule code for embedding is generated by following functions.

$$r^{(k_{z_{12}})} \equiv \begin{cases} 00 & k_{z_{12}}^* = 0 \\ 01 & k_{z_{12}}^* = 1 \\ 10 & k_{z_{12}}^* = 2 \\ 11 & k_{z_{12}}^* = 3 \end{cases}, \quad (10)$$

$$r^{(k_{z_{21}})} = \begin{cases} 00 & k_{z_{21}}^* = 0 \\ 01 & k_{z_{21}}^* = 1 \\ 10 & k_{z_{21}}^* = 2 \\ 11 & k_{z_{21}}^* = 3 \end{cases}, \quad (11)$$

$$r^{(k_{z_{22}})} = \begin{cases} 00 & k_{z_{22}}^* = 0 \\ 01 & k_{z_{22}}^* = 1 \\ 10 & k_{z_{22}}^* = 2 \\ 11 & k_{z_{22}}^* = 3 \end{cases}. \quad (12)$$

Each code is represented in two bit, and embedded into lower two bit on RGB component of the actual pixel \vec{x}_s . After the fuzzy rule embedding, a fuzzy rule embedded reduction image is obtained by using NNI same as the fundamental method.

3.2 Image Enlargement Process

In the enlargement process, light gray pixels in Fig.4 are defined as interpolation target pixels. First, embedded fuzzy rule codes are extracted from lower 2 bit of RGB components of the actual pixel \vec{x}_s . Then, outputs of the proposed fuzzy rules z_{12} , z_{21} and z_{22} in Eq.8 are calculated by the extracted fuzzy rule codes.

$$z_{12} = \begin{cases} \vec{x}_s & r^{(k_{z_{12}})} = 00 \\ \frac{2}{3}\vec{x}_s + \frac{1}{3}\vec{x}_t & r^{(k_{z_{12}})} = 01 \\ \frac{1}{3}\vec{x}_s + \frac{2}{3}\vec{x}_t & r^{(k_{z_{12}})} = 10 \\ \vec{x}_t & r^{(k_{z_{12}})} = 11 \end{cases}, \quad (13)$$

$$z_{21} = \begin{cases} \vec{x}_s & r^{(k_{z_{21}})} = 00 \\ \frac{2}{3}\vec{x}_s + \frac{1}{3}\vec{x}_u & r^{(k_{z_{21}})} = 01 \\ \frac{1}{3}\vec{x}_s + \frac{2}{3}\vec{x}_u & r^{(k_{z_{21}})} = 10 \\ \vec{x}_u & r^{(k_{z_{21}})} = 11 \end{cases}, \quad (14)$$

$$z_{22} = \begin{cases} \vec{x}_s & r^{(k_{z_{22}})} = 00 \\ \frac{2}{3}\vec{x}_s + \frac{1}{3}\vec{x}_v & r^{(k_{z_{22}})} = 01 \\ \frac{1}{3}\vec{x}_s + \frac{2}{3}\vec{x}_v & r^{(k_{z_{22}})} = 10 \\ \vec{x}_v & r^{(k_{z_{22}})} = 11 \end{cases}. \quad (15)$$

After that, each interpolation target pixel value is calculated by the proposed fuzzy rules using Sugeno-Type fuzzy inference (Sugeno, 1985), (Takagi and Sugeno, 1985). The firing strength is

$$w_i = \min(\mu_{1*}(x_1), \mu_{2*}(x_2)), \quad (16)$$

where, $\mu_{1,2*}(\cdot)$ ($*$ = 1 or 2 or 3) are the membership functions for first and second inputs in the proposed fuzzy rule in Eq.8 and Fig.5. The interpolation target pixel value is computed as the weighted average of all rule outputs,

$$\vec{x}_{target} = \frac{\sum_{i=1}^7 w_i z_i}{\sum_{i=1}^7 w_i}, \quad (17)$$

where, z_i is the output of i -th rule in Eq.8 and it is extracted from the embedded code. Finally, the lower 2 bit of R, G and B components change its value to "10", similar to the fundamental method.

4 EXPERIMENTAL RESULTS

To show the effectiveness and validity of the proposed method, we compared the enlarged results of the proposed method with three conventional enlargement methods, NNI, BCI (Lin, 1990) and Nonlinear Extrapolation method (NE) (Greenspan et al., 2000). BCI and NE are selected as the most well-known interpolation and high-frequency-component-enhancement-based enlargement methods, respectively. In our experiments, we use images (512×512 pixels) selected from the SIDBA database, which are royalty-free and have been used in other computer graphics performance tests, and are often referred to as "standard images".

4.1 Objective Evaluation

Error measures are used to objectively compare the enlarged image with the original one, as shown in

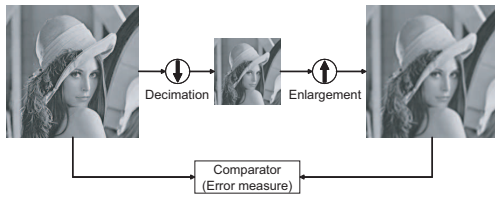


Figure 6: Error measurement for objective evaluation.

Table 1: Result of MSE evaluation (factor = 3)

	NNI	BCI	NE	Proposed
Airplane	355.5	265.2	107.9	53.9
House	486.6	377.9	184.9	139.8
Lenna	223.9	162.9	60.8	59.8
Mandrill	1068.8	871.1	490.5	458.6
Pepper	335.2	251.4	95.0	82.4
Sailboat	557.6	414.2	179.0	167.0
Splash	198.4	149.4	56.8	33.0
Tiffany	231.9	189.4	90.4	58.9
Average	432.2	335.2	158.2	131.7

Table 2: Result of MSE evaluation (factor = 4)

	NNI	BCI	NE	Proposed
Airplane	524.4	401.1	161.0	104.5
House	765.2	609.5	266.7	207.0
Lenna	338.5	251.7	90.8	71.7
Mandrill	1289.9	1061.5	600.1	566.2
Pepper	507.2	384.9	132.2	108.7
Sailboat	808.0	613.9	251.1	195.1
Splash	308.4	238.7	83.1	80.9
Tiffany	309.3	251.1	115.2	113.2
Average	606.4	476.6	212.5	180.8



Figure 7: Results of data embedding; (a) Original and (b) Data embedded image (MSE=16.83).

Fig.6. First, the original image is decimated by a factor of three or four and then enlarged by the same factor. Next, the original and enlarged images are compared using an error measure. In this evaluation, we employ same method to reduction and enlargement process for fair comparison. As an error measure, the mean-squared error (MSE) is used in this paper. The MSE is simply the mean of the squared differences for every channel for every pixel. The MSE can be obtained by the following equation:

$$MSE = \frac{1}{3MN} \sum_{k=R,G,B} \sum_{i=1}^M \sum_{j=1}^N (f_k(i,j) - g_k(i,j))^2. \quad (18)$$

Here, f and g show the original and the enlarged image, respectively. M and N show the number of pixels in horizontal and vertical axis of the image, and $R, G,$ and B show the color component.

Tables 1 and 2 show the result of MSE evaluation among four methods. The results show that the proposed method achieved drastically better performance than the conventional methods.

4.2 Subjective Evaluation

The proposed method changes lower two bit of RGB components of the original image to embed the fuzzy rule code. Therefore, by comparing the original and the fuzzy-rule-embedded image, there is a little error between them but its effect would be limited.

Figure 7 shows an original (before data embedding) and a fuzzy-rule embedded images of “Pepper”. From the results of data embedding shown in Fig.7,

we cannot find the difference between them perceptually. Therefore, we confirm that the data embedding affects quite little modification on the reduction image, from the subjective evaluation.

In Table2, MSE evaluation of NE was nearly equal to the proposed method on images “Splash” and “Tiffany”. Therefore, we select the image “Splash” as for subjective evaluation on enlarged image.

Figure 8 shows part of enlargement results on “Splash”. The enlarged result of NNI generated a quite coarse image around edge area. The result of BCI showed a blurred image. Although the result of NE was better than NNI and BCI, there are many artifacts in the enlarged image. The result of proposed method showed a smooth and sharp image around edge area and achieved better performance than the conventional methods under the subjective evaluation.

5 CONCLUSIONS

In this paper, we propose a fuzzy-rule-embedded reduction image construction method which utilizes for high-quality image enlargement. The proposed method realized high-quality image enlargement in terms of both objective and subjective evaluations in comparison with conventional methods.

In future work, we will combine the proposed

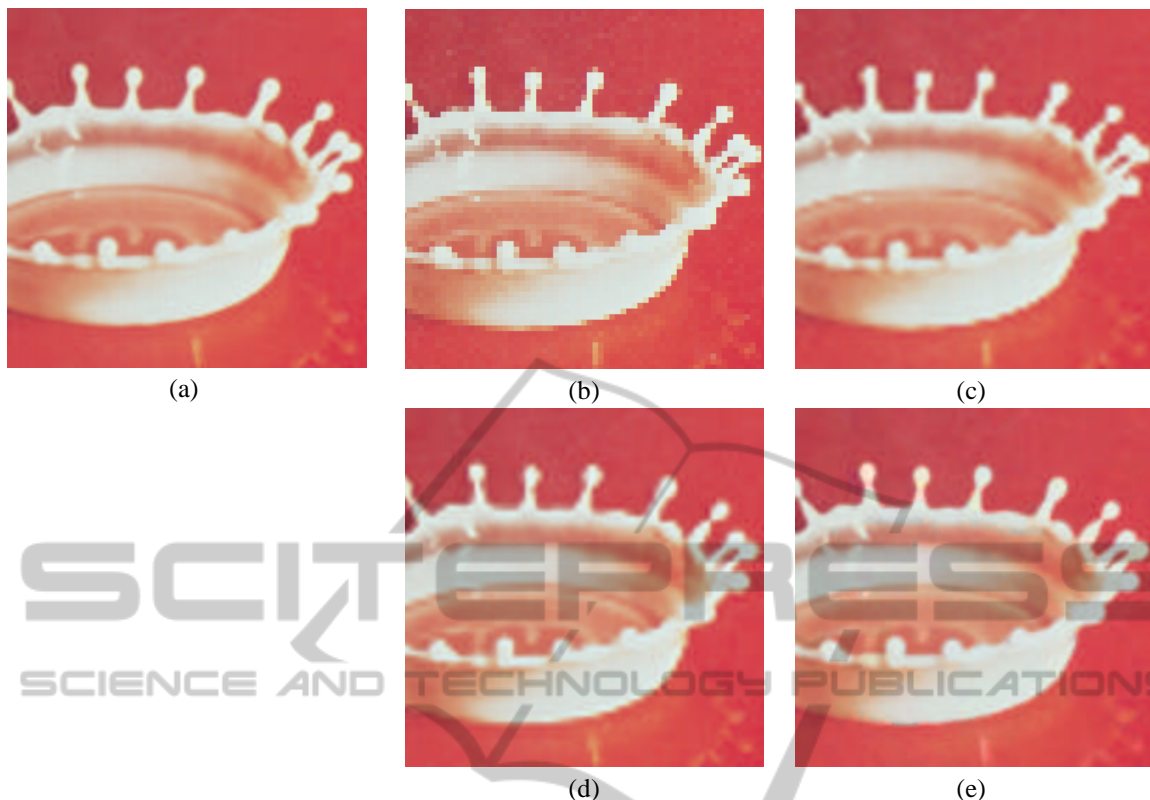


Figure 8: Results of image enlargement (factor = 4) : (a) OriginalC(b) NNIC(c) BCIC(d) NEC(e) Proposed.

method with the other image super resolution methods to improve image quality. After that, we implement it onto a field programmable gate array to realize a real-time and high-quality video enlargement.

ACKNOWLEDGEMENTS

This work was supported by JSPS KAKENHI Grant Number 24300092.

REFERENCES

- Farsiu, S., Robinson, M., Elad, M., and Milanfar, P. (2004). Fast and robust multiframe super resolution. In *IEEE Trans. Image Process.*, volume 13, pages 1327–1344.
- Greenspan, H., Anderson, C. H., and Akber, S. (2000). Image enhancement by nonlinear extrapolation in frequency space. In *IEEE Trans. Image Process.*, volume 9, pages 1035–1048.
- Keys, R. G. (1981). Cubic convolution interpolation for digital image processing. In *IEEE Trans. Acoust. Speech Signal Process.*, volume 26, pages 1153–1160.
- Lin, J. S. (1990). *Two-dimensional signal processing and image processing*. Prentice-Hall, Inc., Upper Saddle River, NJ, USA, 1st edition.
- Siu, W. C. and Hung, K. W. (2012). Review of image interpolation and super-resolution. In *Proc. of Asia-Pacific Signal and Information Processing Association Annual Summit and Conference*, pages 1–10.
- Sugeno, M. (1985). *Industrial applications of fuzzy control*. Elsevier Science Pub. Co.
- Takagi, T. and Sugeno, M. (1985). Fuzzy identification of systems and its applications to modeling and control. In *IEEE Trans. Systems, Man and Cybernetics*, volume 15, pages 116–132.
- Tamukoh, H., Kawano, H., Suetake, N., Sekine, M., Cha, B., and Aso, T. (2013). A data embedded reduction image generation method for high-quality image enlargement. In *Proc. of 7th Int. Conf. on Circuits, Systems, Signal and Telecommunications*, pages 37–42.